Effects of changes in the chain conformation on the kinetics of order-disorder transitions in block copolymer melts

Toshihiro Kawakatsu
Department of Physics, Faculty of Science, Tokyo Metropolitan University, Hachioji, Tokyo 192-03, Japan
(Received 23 December 1996)

The effects of long-range dynamical correlation in the kinetics of order-disorder transitions of symmetric block copolymer melts are investigated on the basis of the time-dependent Ginzburg-Landau model that was extended in such a way that the information on the chain conformation is incorporated using the path-integral formalism. A simplified equation of motion for the order parameter is derived by a perturbation expansion of the chain conformation around its Gaussian conformation. A series of computer simulations are performed to show the importance of the effects of the changes in the chain conformation on the kinetics of order-disorder transition of block copolymer melts. [S1063-651X(97)04309-2]

PACS number(s): 82.20.Wt, 64.60.Ht, 83.10.Nn

I. INTRODUCTION

Research on complex fluids, such as polymers, emulsions, and colloidal suspensions, is now one of the most active fields in computational condensed-matter physics [1,2]. A common feature of these materials is the existence of mesoscopic structures that are much larger than the microscopic atomic length scale but much smaller than the macroscopic length scale. In the microscopic length scale, the materials are described using discrete atomic or molecular degrees of freedom. On the other hand, in the macroscopic length scale, the materials are treated as continuum media. The length scale of the various supermolecular structures in complex fluids is located between these two limiting length scales. The main difficulty in performing computer simulations of complex fluids using the microscopic description comes from the extremely long characteristic time scales of the relaxation of these mesoscopic structures. This difficulty requires us to construct models that are based on the mesoscopic or macroscopic level rather than the microscopic level. A typical example of mesoscopic models of complex fluids is the Ginzburg-Landau model, where the mesoscopic structures are described by coarse-grained density variables or hydrodynamic variables [3,4]. There seems to be a gap between the microscopic approaches, such as the molecular-dynamics method, and the above-mentioned mesoscopic approaches. The purpose of the present study is to try to bridge such a gap by incorporating microscopic information into the mesoscopic models.

II. MODEL

A. Basic equations

As a typical example of problems of complex fluids, we consider phase separation dynamics or dynamics associated with the order-disorder transitions of polymer or block copolymer systems. The block copolymer is a polymer that is composed of two or more different types of polymer chains. Such a molecular structure assigns the block copolymer the amphiphilic nature and therefore the block copolymer plays the role of a surfactant in binary mixtures [4]. The time-dependent Ginzburg-Landau (TDGL) model of phase separation of a polymer blend or a block copolymer melt is given by the equation of motion [5,6]

$$\frac{\partial}{\partial t}\phi_K(\mathbf{r},t)=\sum_{K'}\int d\mathbf{r}'\,\hat{\Lambda}_{KK'}(\mathbf{r},\mathbf{r}')\frac{\delta F}{\delta\phi_{K'}(\mathbf{r}')}, \tag{1}$$

where $\phi_K(\mathbf{r},t)$ is the local number density of K-type segments, K being the index of each component. F and $\hat{\Lambda}_{KK'}(\mathbf{r},\mathbf{r}')$ are the total free energy and the kinetic coefficient, respectively, both of which in general depend on the conformation of the polymer chains.

On the other hand, the conformation of a tagged chain of K type can be calculated within the mean-field approximation (MFA) using the path-integral formalism [7–10]

$$Q_K(\tau,\mathbf{r};\tau',\mathbf{r}')\equiv\sum_{\text{all conformations}}\exp[-\beta(H_0^{(K)}+H_1^{(K)})], \tag{2}$$

where $\beta=1/T$ is the inverse temperature and $Q_K(\tau,\mathbf{r};\tau',\mathbf{r}')$ is the joint probability that the τth segment and the τ'th segment of a K-type chain are found at positions $\mathbf{r}$ and $\mathbf{r}'$, respectively. The right-hand side is a sum of Boltzmann factors for all possible chain conformations under some external constraints, where $H_0^{(K)}$ is the Hamiltonian of an ideal Gaussian chain of K type and $H_1^{(K)}$ is the interaction potential between the monomers of the tagged chain of K type and the self-consistent external field imposed on the monomers. $H_0^{(K)}$ and $H_1^{(K)}$ are usually taken in the forms [11]

$$H_0^{(K)}=\int_0^{N_K}d\tau\left[\frac{dT}{2b^2}\left(\frac{d\mathbf{r}^{(K)}(\tau)}{d\tau}\right)^2\right], \tag{3}$$

$$H_1^{(K)}=\int_0^{N_K}d\tau V_K(\mathbf{r}^{(K)}(\tau)). \tag{4}$$

Here N_K is the total number of segments in a K-type chain, b is the Kuhn statistical length, $\mathbf{r}^{(K)}(\tau)$ is the position of the

τth segment of a K-type chain, $V_K(\mathbf{r})$ is the external field imposed on the K-type segment at position $\mathbf{r}$, and d is the dimensionality of the system that is assumed to be 3 in the following, except for the computer simulations. It is useful to show that the path integral Q_K obeys the diffusion equation [7–10]

$$\frac{\partial}{\partial \tau} Q_K(\tau,\mathbf{r};\tau',\mathbf{r}') = \left[\frac{b^2}{6}\nabla^2 - \beta V_K(\mathbf{r})\right] Q_K(\tau,\mathbf{r};\tau',\mathbf{r}'). \tag{5}$$

As the quantity Q_K is a sum of contributions from all possible polymer conformations (which can be identified with possible paths of a quantum particle moving in a potential V_K), Q_K is called the path integral. Then the free energy F and the kinetic coefficient $\hat{\Lambda}_{KK'}$ in Eq. (1) are calculated using this path integral Q. The free-energy functional at equilibrium is given by [10]

$$F = -T\sum_K \ln\left[\int d\mathbf{r}\int d\mathbf{r}' Q_K(0,\mathbf{r};N,\mathbf{r}')\right] + W[\{\phi_K(\mathbf{r})\}] - \sum_K \int d\mathbf{r}\left[\frac{\delta W}{\delta \phi_K(\mathbf{r})}\phi_K(\mathbf{r}) + U(\mathbf{r})\phi_K(\mathbf{r})\right], \tag{6}$$

where $W[\{\phi_K\}]$ is the interaction energy between segments and $U(\mathbf{r})$ is the Lagrange multiplier for the incompressibility condition

$$\sum_K \phi_K(\mathbf{r}) = \phi_0 = \frac{1}{b^d} = \text{const.} \tag{7}$$

On the right-hand side of Eq. (6), the first and the second terms are the conformational entropy of the chains and the direct segment-segment interaction, respectively. The last term is the correction for the double counting of the segment-segment interaction. This path-integral formalism within the MFA has been used widely and successfully to study equilibrium phase-separated structures in polymer blends and block copolymer systems [8–10,12,13]. A difficulty of this approach comes from the heavy computer demands that are necessary in evaluating the path integral.

In the vicinity of the critical point of the phase separation or the order-disorder transition point, there is an approximated method to evaluate the free energy F by expanding it into a power series in the density fields $\{\phi_K(\mathbf{r})\}$ and by relating the expansion coefficients to the density-density correlation functions that can be calculated using the random-phase approximation (RPA) [14,15]. As shown by Fredrickson and Helfand [16] and by Fried and Binder [17,18], the use of the RPA is restricted to the weak segregation regime (close to the critical point) of systems composed of long chains. Unless the above conditions are satisfied, corrections to the RPA cannot be negligible. Thus, in order to give a quantitative prediction of the phase-separated structures within the MFA, we should restrict ourselves to one of the following situations: (i) The chain length is sufficiently long and the system is close enough to the critical point so that both the use of the RPA and the power-series expansion of the free energy with respect to the density field are valid or (ii) the system is far from the critical point and the chain length is long enough so that the path-integral description and the use of the Gaussian statistics (3) is justified. In this case, a direct numerical evaluation of the path integral (2) is necessary.

Apart from the equilibrium properties, the dynamic properties of phase-separation processes are also interesting and important in predicting the metastable phase-separated domain structures that contain many defects and in predicting the macroscopic rheological properties. In this case, the information on the chain conformation can be incorporated by combining the dynamical equation of motion (1) with the free-energy functional calculated with the path integral (6). Such a trial has started only recently [19–22]. However, in the dynamical modeling, a careful treatment of the kinetic coefficient $\hat{\Lambda}_{KK'}$ is required. As the kinetic coefficient contains effects of segment diffusion, the hydrodynamic interaction, and other dynamical processes, it is very complex. In dynamical simulations of the phase-separation processes using the Ginzburg-Landau-type models, the kinetic coefficient $\hat{\Lambda}_{KK'}$ almost always has been approximated by a local diffusion process where $\hat{\Lambda}_{KK'}$ is replaced by $L\nabla\delta(\mathbf{r}-\mathbf{r}')\nabla'$, L being the diffusion constant [23–25], or approximated by a sum of the local diffusion and a hydrodynamic correlation that is described using the so-called Oseen tensor [26]. However, basically the kinetic processes such as segment diffusion and hydrodynamic processes are affected by the changes in the conformation of constituent polymer molecules. This leads to a nonlocal kinetic coefficient $\hat{\Lambda}_{KK'}$ that depends on the chain conformation through the path integral $Q(\tau,\mathbf{r};\tau',\mathbf{r}')$.

In order to incorporate such nonlocal effects in the kinetic coefficient into the model, one possible way is to use dynamical models of coarse-grained multichain systems and to perform Monte Carlo or molecular-dynamics simulations [27]. In these models, the system is composed of many chains, each of which is treated as a set of many beads connected by chemical bondings, and therefore the models are rather on the microscopic basis than the Ginzburg-Landau-type continuum models. The Monte Carlo simulation by Sariban and Binder showed that the changes in the chain conformation do take place in the course of the phase separation of a binary polymer mixture in a common solvent [27]. On the other hand, on the level of the Ginzburg-Landau-type descriptions, a model of nonlocal kinetic coefficients has been proposed assuming biased reptation dynamics [5,6], where the chains are allowed to diffuse only along its contour because the chains cannot cross each other. This assumption leads to a picture of long-range hopping of a segment from one end of the chain to the other end. (In the case of a diblock copolymer, a segment at one end is regarded to jump to the junction point and simultaneously the segment at the junction point is regarded to jump to the other end.) This picture is, of course, too simple to describe the chain dynamics in real polymer systems, especially in a melt state where the reptation motion should be accompanied by a relaxation of fluctuations in a segment density distribution. Another difficulty of this picture is the fact that, in the case of a strongly segregated block copolymer melt, the junction

points are almost pinned at interfaces, which leads to an extremely slow reptation motion compared to that assumed in the above picture [28]. However, such a simple picture is still a useful and tractable starting point in examining how much the change in the chain conformation is important in the dynamics of phase-separation of polymer systems.

Only very few numerical works have been done on such phase-separation dynamics on the basis of the TDGL-type description with nonlocal kinetic coefficient that depends on the chain conformation. Kawasaki and Koga [29] simulated a phase-separation process of binary polymer blend where the nonlocal kinetic coefficient $\hat{\Lambda}_{KK'}(\mathbf{r}-\mathbf{r}')$ is assumed to be constant within a certain range that models a nondeformed Gaussian chain. However, the assumption of nondeformed chains is not justified for chains that locate in the interfacial region or in the microphase-separated block copolymer systems [8,27]. In such regions, the chains are elongated or compressed by the interaction between segments and by the constraint force originating from the incompressibility condition.

The aim of the present study is to estimate the effects of changes in the chain conformation on the phase-separation dynamics and to show the importance of incorporating the information on the chain conformation into mesoscopic models such as the TDGL model described by Eq. (1), where both the kinetic coefficient $\hat{\Lambda}_{KK'}$ and the free energy F depend on the chain conformation through the path integral Q. As the self-consistent field in $H_1^{(K)}$ depends on the local monomer densities $\{\phi_K(\mathbf{r})\}$, Eqs. (1) and (2) form a set of self-consistent equations. The dependence of the free energy on the chain conformation will be reported elsewhere [21,22] and we will concentrate on the kinetic coefficient in the present study.

Note that there is a similarity between the above formulation for polymer systems and the formulation adopted in the first-principles molecular-dynamics simulations for atomic systems, which is known as the Car-Parrinello (CP) method [30]. In the CP method, the density distributions of valence electrons are obtained at every simulation time step by solving a self-consistent equation for the wave functions of the electrons that are equilibrated in the potential exerted by the atomic ion cores. In this CP method, the ion cores are treated as classical objects, while the electrons are treated as quantum objects. In our polymer formulation, the path integral Q in Eq. (2) corresponds to the wave function of the electrons in the CP method and the segment density distributions $\{\phi_K\}$ correspond to the classical degrees of freedom, respectively.

B. Perturbation expansion

When one wants to simulate the temporal evolution of the phase separation of a polymer mixture taking the effects of the conformational change of the constituent polymer chains into account, one should solve the self-consistent set of equations (1) and (2) directly, by a numerical integration method. Such a numerical procedure requires enormous computer power and is not an easy task even for a two-dimensional system. Thus it is important to estimate the effects of the conformational changes before performing the full numerical simulation of Eqs. (1) and (2). In the present study, we adopt a perturbation expansion of the chain conformation around the Gaussian conformation as a reference state.

It is well known for melts of sufficiently long polymer chains that the polymer chain conformation is Gaussian when there are no density fluctuations and composition fluctuations. Such a Gaussian conformation is actually a solution of Eq. (5) when there is no external field V_K. As the conformational change of the polymer chain from its Gaussian conformation is caused by the external field V_K, the conformational change can be treated as a series of perturbation expansion with respect to V_K that is related to the segment density distribution $\{\phi_K\}$. Here we show such a perturbation expansion using a symmetric block copolymer melt as an example.

We will adopt the RPA in order to evaluate the expansion coefficients of the above-mentioned perturbation expansion. As discussed in the Sec. II A, the use of the RPA becomes unreliable in the short chain limit [16–18]. Due to this problem, the following treatment should be restricted to the case with relatively long chain length and close enough to the critical point.

Let us consider an A-B-type symmetric block copolymer melt that is composed of $N/2$ segments of A type and $N/2$ segments of B type. Each segment is labeled by an index τ so that $0 \leqslant \tau \leqslant N/2$ corresponds to the A subchain and $N/2 \leqslant \tau \leqslant N$ corresponds to the B subchain, respectively. Following Ref. [6], the nonlocal kinetic coefficient $\hat{\Lambda}_{KK'}(\mathbf{r},\mathbf{r}')$ in Eq. (1) is related to the two segment correlation function

$$P_{\tau,\tau'}(\mathbf{r},\mathbf{r}') = n_0 \langle \delta(\mathbf{r}-\mathbf{r}(\tau))\delta(\mathbf{r}'-\mathbf{r}(\tau')); \{\phi_K(\mathbf{r})\}\rangle, \quad (8)$$

where n_0 is the total number of chains in the system, $\mathbf{r}(\tau)$ and $\mathbf{r}(\tau')$ are the positions of τth and τ'th segments of a tagged chain, and the average $\langle *; \{\phi_K(\mathbf{r})\}\rangle$ is the canonical average under the condition that the density distributions are fixed to $\{\phi_K(\mathbf{r})\}$.

Using $P_{\tau,\tau'}(\mathbf{r},\mathbf{r}')$, the TDGL equation (1) is rewritten as

$$\frac{\partial}{\partial t}\phi_K(\mathbf{r}) = -\frac{D_c}{T}\sum_{K'} \int d\mathbf{r}' \overline{P}_{KK'}(\mathbf{r},\mathbf{r}') \frac{\delta F}{\delta \phi_{K'}(\mathbf{r}')}, \quad (9)$$

where D_c is the diffusion constant along the chain due to the reptation motion, T is the temperature, and $\overline{P}_{KK'}(\mathbf{r},\mathbf{r}')$ is defined by

$$\overline{P}_{KK'}(\mathbf{r},\mathbf{r}') = \int_{\omega_K} d\tau \int_{\omega_{K'}} d\tau' \frac{\partial^2}{\partial\tau\partial\tau'} P_{\tau\tau'}(\mathbf{r},\mathbf{r}'), \quad (10)$$

where the integral $\int_{\omega_K} d\tau$ is taken over the K-type subchain of the tagged chain. In deriving Eq. (9), we assumed biased reptation motion of the chains [5,6].

The incompressibility condition (7) introduces a Lagrange multiplier $U(\mathbf{r})$ and $\delta F/\delta\phi_K$ in Eq. (9) should be replaced by $\delta F/\delta\phi_K + U$. Eliminating this Lagrange multiplier $U(\mathbf{r})$ using the incompressibility condition (7), we obtain for melts of A-B binary systems (including A-B-type block copolymer melts)

$$\frac{\partial}{\partial t}X(\mathbf{r},t)=\frac{2D_c}{T}\int d\mathbf{r}'\,\Lambda(\mathbf{r},\mathbf{r}')\frac{\delta F}{\delta X(\mathbf{r}')}, \tag{11}$$

where

$$X(\mathbf{r},t)=\phi_A(\mathbf{r},t)-\phi_B(\mathbf{r},t) \tag{12}$$

is the order parameter of the phase separation and

$$\frac{\delta F}{\delta X}=\frac{\delta F}{\delta \phi_A}-\frac{\delta F}{\delta \phi_B} \tag{13}$$

is the chemical potential difference of an A segment and a B segment, which plays the role of the thermodynamic force for the order parameter. For an A-B symmetric block copolymer melt, Λ is given in the Fourier space as

$$\Lambda(\mathbf{q},\mathbf{q}')=\frac{1}{\sum_K\sum_{K'}\overline{P}_{KK'}}(\overline{P}_{AA}\overline{P}_{BB}-\overline{P}_{AB}\overline{P}_{BA}). \tag{14}$$

For a symmetric A-B block copolymer of length N, $\overline{P}_{KK'}$ defined by Eq. (10) is simplified to

$$\begin{aligned}
\overline{P}_{AA}&=P_{00}+P_{(N/2)(N/2)}-P_{0(N/2)}-P_{(N/2)0},\\
P_{AB}&=P_{0(N/2)}+P_{(N/2)N}-P_{0N}-P_{(N/2)(N/2)},\\
P_{BA}&=P_{(N/2)0}+P_{N(N/2)}-P_{N0}-P_{(N/2)(N/2)},\\
P_{BB}&=P_{(N/2)(N/2)}+P_{NN}-P_{(N/2)N}-P_{N(N/2)}.
\end{aligned} \tag{15}$$

The above set of $\{\overline{P}_{KK'}\}$ describes the fact that within the level of our assumption of biased reptation of a diblock copolymer chain, one end segment ($\tau=0$ or $\tau=N$) can be regarded to hop to the position of the junction segment ($\tau=N/2$) and the junction segment hops to the other end position ($\tau=N$ or $\tau=0$) due to the sliding motion of the chain along its contour.

As a lowest-order approximation, we can use Gaussian distribution of the chain conformation. Within this approximation, the Fourier transform of $\Lambda(\mathbf{r},\mathbf{r}')$ leads to [6]

$$\Lambda_0(\mathbf{q},\mathbf{q}')=\frac{n_0(2\pi)^d}{2V}\{4\eta_{N/2}(\mathbf{q})-\eta_N(\mathbf{q})\}\delta(\mathbf{q}+\mathbf{q}'), \tag{16}$$

where V is the system volume and $\eta_\tau(\mathbf{q})$ is defined for the three-dimensional system as

$$\eta_\tau(\mathbf{q})=1-\exp(-\tfrac{1}{6}\tau b^2q^2) \tag{17}$$

or in the real space as

$$\eta_\tau(\mathbf{r})=\delta(\mathbf{r})-\left(\frac{3}{2\pi b^2\tau}\right)^{3/2}\exp\left[-\frac{3|\mathbf{r}|^2}{2b^2\tau}\right]. \tag{18}$$

Under the existence of the inhomogeneity of the density distribution, the block copolymer chains are deformed and therefore the chain conformation deviates from the Gaussian conformation. We incorporate such an effect by a perturbation expansion. For a tagged block copolymer chain in the external field induced by the surrounding segment distributions that are described by the order parameter $X(\mathbf{r})$, the path integral defined by Eq. (2) is expressed as

$$Q_K(\tau,\mathbf{r};\tau,\mathbf{r}')=\int\delta\{\mathbf{r}(\tau)\}\exp[-\beta(H_0+H_1)], \tag{19}$$

where H_0 and H_1 are now rewritten as

$$\begin{aligned}
H_0&=\int_0^N d\tau\left[\frac{dT}{2b^2}\left(\frac{d\mathbf{r}(\tau)}{d\tau}\right)^2\right]\\
H_1&=\int_0^{N/2}d\tau[w_A(\mathbf{r}(\tau))+U_A(\mathbf{r}(\tau))]\\
&\quad+\int_{N/2}^N d\tau[w_B(\mathbf{r}(\tau))+U_B(\mathbf{r}(\tau))].
\end{aligned} \tag{20}$$

Here $w_K(\mathbf{r})$ is the segment-segment direct interactions given by

$$\begin{aligned}
w_K(\mathbf{r})&=-\frac{z}{2}[\epsilon_{KA}\phi_A(\mathbf{r})+\epsilon_{KB}\phi_B(\mathbf{r})]\\
&=-\frac{z}{2}(\epsilon_{KA}-\epsilon_{KB})X(\mathbf{r})+\text{const}
\end{aligned} \tag{21}$$

and $U_A(\mathbf{r})$ and $U_B(\mathbf{r})$ are the Lagrange multipliers coming from the constraint that the density profiles ϕ_A and ϕ_B satisfy the relations

$$\phi_A(\mathbf{r})+\phi_B(\mathbf{r})=\phi_0,\quad \phi_A(\mathbf{r})-\phi_B(\mathbf{r})=X(\mathbf{r}), \tag{22}$$

where ϕ_0 is the total segment density that is assumed to be constant and the order parameter $X(\mathbf{r})$ is regarded as an external parameter to which the segment distribution calculated with the path integral (19) should be adjusted. Using these constraints, we can determine the Lagrange multipliers U_A and U_B. Then the expression of H_1 leads to

$$\begin{aligned}
H_1&=-\frac{1}{2\beta}\int_0^{N/2}d\tau\int d\mathbf{r}'\,G(\mathbf{r}(\tau)-\mathbf{r}')X(\mathbf{r}')\\
&\quad+\frac{1}{2\beta}\int_{N/2}^N d\tau\int d\mathbf{r}'\,G(\mathbf{r}(\tau)-\mathbf{r}')X(\mathbf{r}')\\
&=\int_0^N d\tau f(\tau)\psi(\mathbf{r}(\tau)),
\end{aligned} \tag{23}$$

where we have defined

$$\psi(\mathbf{r}) = -\frac{1}{2\beta}\int d\mathbf{r}' G(\mathbf{r}-\mathbf{r}')X(\mathbf{r}'), \tag{24}$$

$$f(\tau) = \begin{cases} 1 & (0 \leqslant \tau \leqslant N/2) \\ -1 & (N/2 \leqslant \tau \leqslant N). \end{cases} \tag{25}$$

$G(\mathbf{q})$ is the Fourier transform of the two-point density correlation function, whose explicit expression can be obtained within the RPA as

$$G(\mathbf{q}) = \frac{b^d x^2}{N(x+4e^{-x/2}-e^{-x}-3)}, \tag{26}$$

where $x=(1/6)Nb^2|\mathbf{q}|^2$ and the factor b^d is the inverse of the total segment number density (7). Using the path integral (19), one can calculate $P_{\tau\tau'}(\mathbf{r},\mathbf{r}')$ in Eq. (8) by

$$P_{\tau\tau'}(\mathbf{r},\mathbf{r}') = n_0 \frac{\int \delta\{\mathbf{r}(\tau)\}\delta(\mathbf{r}(\tau)-\mathbf{r})\delta(\mathbf{r}(\tau')-\mathbf{r}')\exp[-\beta(H_0+H_1)]}{\int \delta\{\mathbf{r}(\tau)\}\exp[-\beta(H_0+H_1)]}. \tag{27}$$

In order to evaluate Eq. (27) directly, we have to rely on an extensive numerical calculation. Here we instead expand Eq. (27) in a power series in H_1 and retain terms up to second order. As the details of such a perturbation expansion are described in the Appendix, here we summarize the results. The zeroth-order terms of the expansion give Eq. (16). We find that the first-order terms vanish exactly. This is due to the special situation of our system of symmetric block copolymers (see the Appendix). Then the first nontrivial contribution arises from the second-order terms. This procedure leads us to a complicated expression for the kinetic coefficient $\Lambda(\mathbf{r})$ in Eq. (11), whose explicit expression in the Fourier space is given in Eq. (A12).

In order to obtain an equation of motion for the order parameter that is convenient for computer simulations, we expand the perturbation terms in $\Lambda(\mathbf{q})$ in a power series in wave numbers anticipating that the perturbation terms are dominated by the long-wavelength fluctuations in the order parameter $X(\mathbf{r})$. Retaining the leading contributions, we finally obtain the modified TDGL equation

$$\frac{\partial}{\partial t}X(\mathbf{r},t) = -\frac{2D_c}{T}\left\{\left(1-\frac{1}{2}\beta^2\langle H_1^2\rangle_0\right)\int d\mathbf{r}'\Lambda_0(\mathbf{r}-\mathbf{r}') \times\frac{\delta F}{\delta X(\mathbf{r}')} - \frac{6b^{2d}n_0}{V}\nabla\cdot\left[|\mathbf{a}(\mathbf{r})|^2\nabla\frac{\delta F}{\delta X(\mathbf{r})}\right]\right\}. \tag{28}$$

In this equation $\Lambda_0(\mathbf{r}-\mathbf{r}')=\Lambda_0(\mathbf{r},\mathbf{r}')$ is the Fourier inverse transform of $\Lambda_0(\mathbf{q},\mathbf{q}')$ defined in Eq. (16) that is the kinetic coefficient for undeformed Gaussian chains, $\eta_\tau(\mathbf{r})$ is defined in Eq. (17), and

$$\mathbf{a}(\mathbf{r}) = \frac{1}{(2\pi)^d}\int d\mathbf{q}e^{-i\mathbf{q}\cdot\mathbf{r}}[-i\mathbf{q}\Omega(\mathbf{q})X(\mathbf{q})] = \nabla\int d\mathbf{r}'\Omega(\mathbf{r}-\mathbf{r}')X(\mathbf{r}'), \tag{29}$$

where $\Omega(\mathbf{r})$ is defined by

$$\Omega(\mathbf{r}) = \frac{1}{(2\pi)^d}\int d\mathbf{q}\,\frac{1}{q^2}e^{-i\mathbf{q}\cdot\mathbf{r}}. \tag{30}$$

The quantity $\langle H_1^2\rangle_0$ is defined in Eq. (A5) and is now expressed in the same level of approximation as

$$\langle H_1^2\rangle_0 = \left(\frac{1}{2\beta}\right)^2\frac{144}{Nb^{2-2d}V}\frac{1}{(2\pi)^d}\int d\mathbf{q}\frac{1}{q^2}|X(\mathbf{q})|^2 = \left(\frac{1}{2\beta}\right)^2\frac{144}{Nb^{2-2d}V}\int d\mathbf{r}\int d\mathbf{r}'\Omega(\mathbf{r}-\mathbf{r}')X(\mathbf{r})X(\mathbf{r}'). \tag{31}$$

Equation (28) is our basic equation used in the analysis in the present work. It can be regarded as a gradient expansion of the original TDGL equation (11).

III. COMPUTER SIMULATION

A. Model equations for computer simulations

In this section we investigate the effects of the conformational changes on the phase-separation dynamics of a dense *A*-*B*-type symmetric block copolymer system using computer simulations on the modified TDGL equation (28). In the present study, we focus our attention on the kinetic coefficient Λ. In order to separate the effects of the conformational changes in the kinetic coefficient from the other effects, we neglect the hydrodynamic effects [26] and viscoelastic effects [31]. For the same reason we adopt a conventional free energy model for the block copolymer melt that is split into two contributions [15,24,25,32]

$$F = F_S + F_L, \tag{32}$$

where F_S and F_L are the short-range part and the long-range part of the free energy. The short-range part is usually as-

sumed to be of the Flory-Huggins type or the Ginzburg-Landau (GL) type. Here we adopt the GL type model given by

$$F_S=\frac{1}{\beta}\int d\mathbf{r}\left[\frac{D}{2}|\nabla X(\mathbf{r})|^2-\frac{c}{2}X^2(\mathbf{r})+\frac{u}{4}X^4(\mathbf{r})\right], \quad (33)$$

where D, c, and u are positive constants. The long-range part is calculated by applying the RPA to Eq. (6) and retaining only the small wave-number contributions. Its explicit expression for a symmetric block copolymer melt is given by [15]

$$F_L=\frac{1}{2\beta}\frac{36}{b^{2-d}N^2}\int d\mathbf{r}\int d\mathbf{r}'\,\Omega(\mathbf{r}-\mathbf{r}')X(\mathbf{r})X(\mathbf{r}'), \quad (34)$$

where $\Omega(\mathbf{r})$ is defined in Eq. (30).

In order to transform the equation of motion into a nondimensional form, we take the units of time t_0, length l_0, energy ϵ_0, and the order parameter X_0 as $t_0=V/n_0D_cc$, $l_0=\sqrt{D/c}\equiv\xi$, $\epsilon_0=1/\beta$, and $X_0=l_0^d\sqrt{c/u}$, respectively. Here ξ corresponds to the correlation length of the phase separation apart from a factor $\sqrt{2}$ and X_0 is the difference between the number of A segments and the number of B segments in a unit volume of ξ^d in a bulk domain in the equilibrium state. The correlation length ξ is determined by the segment-segment interaction parameters and is the same order as the interfacial thickness. Note that ξ is different from the characteristic length of the final microphase separated structure such as the lamellar spacing. Using these units, we obtain

$$\frac{\partial}{\partial t}X(\mathbf{r},t)=-(1-\tfrac{1}{2}\langle H_1^2\rangle_0)\int d\mathbf{r}[4\,\eta_{N/2}(\mathbf{r}-\mathbf{r}')-\eta_N(\mathbf{r}-\mathbf{r}')]\mu(\mathbf{r})+C_1\nabla\cdot[|\mathbf{a}(\mathbf{r})|^2\nabla\mu(\mathbf{r})], \quad (35)$$

where all the quantities are now nondimensional and

$$\eta_N(\mathbf{r})=\delta(\mathbf{r})-\left(\frac{d}{12\pi(R_g/\xi)^2}\right)^{d/2}\exp\left[-\frac{d|\mathbf{r}|^2}{12(R_g/\xi)^2}\right],$$

$$\eta_{N/2}(\mathbf{r})=\delta(\mathbf{r})-\left(\frac{d}{6\pi(R_g/\xi)^2}\right)^{d/2}\exp\left[-\frac{d|\mathbf{r}|^2}{6(R_g/\xi)^2}\right],$$

$$\mu(\mathbf{r})=-\nabla^2X(\mathbf{r})-X(\mathbf{r})+[X(\mathbf{r})]^3+C_2\int d\mathbf{r}'\,\Omega(\mathbf{r}-\mathbf{r}')X(\mathbf{r}'),$$

$$\mathbf{a}(\mathbf{r})=\nabla\int d\mathbf{r}'\,\Omega(\mathbf{r}-\mathbf{r}')X(\mathbf{r}'),$$

$$\langle H_1^2\rangle_0=C_3\int d\mathbf{r}\int d\mathbf{r}'\,\Omega(\mathbf{r}-\mathbf{r}')X(\mathbf{r})X(\mathbf{r}'), \quad (36)$$

where the dimensionality d is set equal to 2 in the simulations. The coefficients are defined by

$$C_1=\left[X_0\left(\frac{b}{\xi}\right)^d\right]^2, \quad C_2=\left(\frac{R_g}{\xi}\right)^{-2}\frac{b^{d+2}}{c},$$

$$C_3=6C_1\left(\frac{R_g}{\xi}\right)^{-2}\frac{\xi^d}{V}, \quad (37)$$

where $R_g=\sqrt{Nb^2/6}$ is the gyration radius of the chain in its Gaussian state. Here we note that C_1 corresponds to the difference between the volume fraction of the A segments and that of the B segments in the equilibrium composition and is therefore less than 1. The parameter C_2 determines the lamellar domain spacing in units of the correlation length ξ. Thus the three dimensionless parameters C_1, C_2, and C_3 can be fixed using the experimental data on the segment volume fraction of the equilibrium composition, the equilibrium lamellar spacing divided by ξ, and the gyration radius divided by ξ, respectively.

B. Simulation techniques

We solved the equation of motion (35)–(37) for a two-dimensional system by numerical integration using the standard Euler difference scheme. The integral on the right-hand side of Eq. (35) extends over a long-range due to the long-range nature of the kinetic coefficient $\Lambda_0(\mathbf{r})$. As this convolution integral is transformed into a simple multiplication in the Fourier space, it is evaluated in the Fourier space at every time step using the fast Fourier transform (FFT) method [26]. This method is also applicable for systems with hydrodynamic interactions [26]. Therefore, the present simulation program is very easily extended to the systems with hydrodynamic interactions by simply adding the Oseen tensor to the kinetic coefficient Λ_0. The same technique is also used for evaluating Eqs. (29) and (31). We neglected the differences in the model parameters between the two-dimensional system (2D) and the three-dimensional system. Although the function $\Omega(\mathbf{r})$ takes different functional forms in 2D and 3D systems, it does not present any difficulty to the present simulation because Ω is evaluated only in the Fourier space where there is no difference in the functional form of $\Omega(\mathbf{q})$ between 2D and 3D systems.

We performed computer simulation runs on the ordering process (microphase-separation process) from a uniformly mixed state of the block copolymer. We set the parameters $C_1=0.1^2$, $C_2=0.01(R_g/\xi)^{-2}$, $C_3=6C_1(R_g/\xi)^{-2}(\xi^d/V)$, and $R_g/\xi=2.0$, 3.0, 4.0, and 5.0, respectively. This selection of the parameter C_1 corresponds to the weak-segregation regime. The system is divided into 128×128 square meshes with a mesh width $\xi=1.0$ and we impose a periodic boundary condition on each side of the system. The time mesh width Δt is taken as $\Delta t=0.01$ for the system with $R_g/\xi=2.0$ and $\Delta t=0.001$ for those with $R_g/\xi>2.0$. Then the equation of motion was integrated up to $t=100.0$. The initial values of the order parameter $X(\mathbf{r})$ at mesh points are generated using independent normal random numbers with mean 0 and standard deviation 0.1. In order to get statisti-

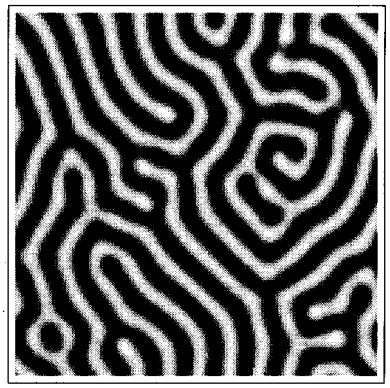

FIG. 1. Picture of the segment density distribution obtained by a simulation on the full equation of motion including perturbation terms. The system is divided in a 128×128 square mesh with a nondimensional unit. The parameters are $C_1=0.1^2$, $C_2=0.01(R_g/\xi)^{-2}$, and $R_g/\xi=2.0$. The time is $t=50.0$.

cally accurate data, we performed ten independent runs from different initial conditions.

C. Kinetics of lamellar ordering from a uniformly mixed state

The effects of the conformational change of the chain, i.e., the perturbation terms in Eq. (35), were investigated by performing two types of simulation runs for each parameter set: one is a simulation on the full equation of motion (35) and the other is a simulation where the perturbation terms in Eq. (35), i.e., the terms containing $\langle H_1^2\rangle_0$ and C_1, are dropped. In Fig. 1 we show a typical picture of the system calculated using the full equation of motion including the perturbation terms. The picture is a snapshot of the system with $R_g/\xi=2.0$ taken at $t=50.0$. The black regions and the white regions correspond to the A domains and B domains of a lamellar structure, respectively. The simulation without the perturbation terms shows a similar domain structure.

The ordering process is characterized by the temporal evolution of the characteristic wave number of the domain structure that is defined by

$$\langle k(t)\rangle=\int_0^\infty kS(k)dk\Big/\int_0^\infty S(k)dk, \tag{38}$$

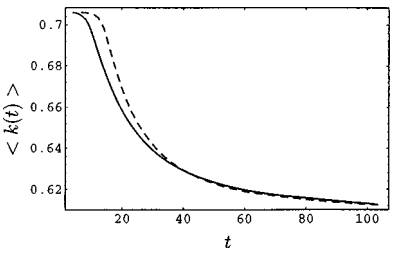

FIG. 3. Same data as in Fig. 2(a), but the unit of time for the dashed curve (the case with the perturbation terms) is properly changed so that the asymptotic behaviors of the two curves fit each other. Obviously, the curves do not fall onto a single master curve in the early stage.

where $S(k)$ is the structure function given by

$$S(k)=\langle|X(\mathbf{k})|^2\rangle, \tag{39}$$

which is a function of $k\equiv|\mathbf{k}|$ for isotropic systems. In Fig. 2 temporal evolution of the characteristic wave number $\langle k(t)\rangle$ is shown as a function of time, where the chain length is taken to be $R_g/\xi=2.0$, 3.0, 4.0, and 5.0 in Figs. 2(a), 2(b), 2(c), and 2(d), respectively. In these figures the results of simulations using the equation of motion without the perturbation terms are shown by solid curves, while those with the full equation of motion including the perturbation terms are shown by dashed curves. We observe a non-negligible contribution from the perturbation terms that accelerates the ordering process, especially in the early stage. We also notice that the contribution of the perturbation terms becomes larger when the chain length becomes longer. Here it should be noted that the equilibrium lamellar domain sizes of these four cases (a)–(d) are different because of the difference in the chain lengths. Moreover, the unit time scale $t_0=V/n_0D_cc$ is also different for Figs. 2(a)–2(d) as it is a decreasing function of the chain length. Thus a direct quantitative comparison of the data shown in Figs. 2(a)–2(d) is not appropriate.

One may think that the perturbation effects only changes the rate of the ordering process and the temporal change of the characteristic wave number $\langle k(t)\rangle$ is described by a single scaling function by appropriately choosing the unit of time. We show in Fig. 3, the same data as in Fig. 2(a), but

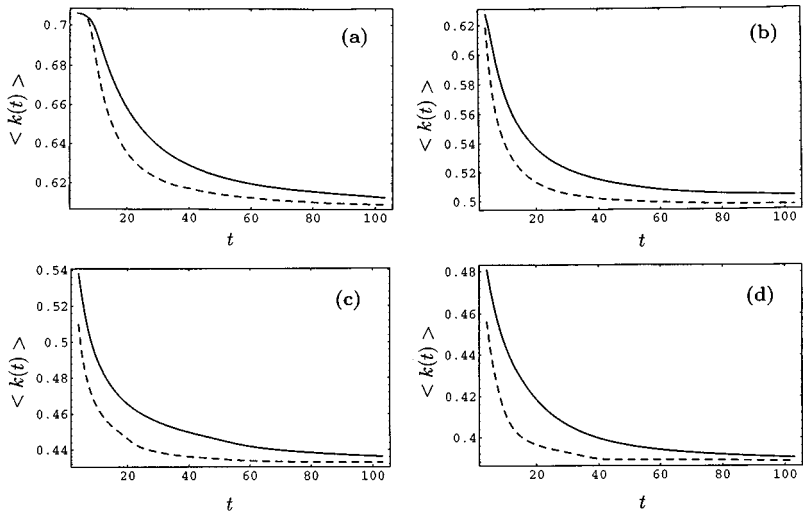

FIG. 2. Comparison of the temporal change of the characteristic wave numbers of the domain structures for the case without the perturbation terms (solid curve) and the case with the perturbation terms (dashed curve) for various values of the chain length: (a) $R_g/\xi=2.0$, (b) $R_g/\xi=3.0$, (c) $R_g/\xi=4.0$, and (d) $R_g/\xi=5.0$, respectively. The other parameters are the same as those in Fig. 1.

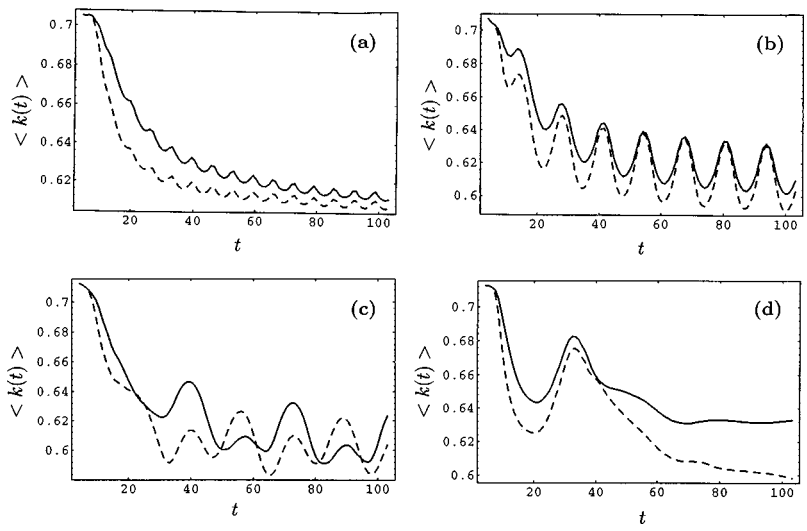

FIG. 4. Comparison of the temporal change of the characteristic wave numbers of the domain structures under an external shear flow. Solid curves show the case without the perturbation terms and the dashed curves show the case with the perturbation terms. The chain length is fixed to be $R_g/\xi=2.0$. The frequency of the oscillation of the shear flow is changed as (a) $\omega=1.0$, (b) $\omega=0.5$, (c) $\omega=0.2$, and (d) $\omega=0.1$, respectively, keeping the parameter $\dot{\gamma}_0=0.1$ constant.

the time scale for the case with the perturbation terms (dashed curve) is extended by a factor 1.70 so that the asymptotic long-time behavior of the solid curve and the dashed curve fit each other. It is obvious that these two curves do not fall onto a single master curve in the early stage. Thus the effects of the perturbation terms are not merely changing the time scale but changing the qualitative behavior of the ordering process in the early stage to the intermediate stage.

D. Kinetics of lamellar ordering under a shear flow

Next we investigate the effects of an external flow field, such as a shear flow. As the shear stress deforms the domain structure, it will cause a stretching of the block copolymer chain. Thus we expect that the external shear flow will enhance the effects of the perturbation terms. We performed a series of simulation runs on the ordering processes under a simple shear flow. In this case, the left-hand side of the equation of motion (35) is modified as [25]

$$\frac{\partial}{\partial t}X(\mathbf{r},t)\Rightarrow\frac{\partial}{\partial t}X(\mathbf{r},t)+\nabla\cdot[\mathbf{v}(\mathbf{r},t)X(\mathbf{r},t)]. \tag{40}$$

As we did in the simulations described in Sec. III C, we neglect the contribution from the hydrodynamic interaction between composition fluctuations at distant points and we assume that the velocity field $\mathbf{v}(\mathbf{r},t)$ is given only by the external shear flow that has the form

$$\mathbf{v}(\mathbf{r},t)=(\dot{\gamma}(y,t)y,0), \tag{41}$$

where $\dot{\gamma}(y,t)$ is the shear rate. The FFT technique that is used in our simulation requires the periodic boundary condition [33]. In order to make the shear flow (41) match the periodic boundary condition, we use the temporary and spatially periodic shear flow

$$\dot{\gamma}(y,t)=\dot{\gamma}_0\sin(2\pi y/L_y)\sin(\omega t), \tag{42}$$

where $\dot{\gamma}_0$ is a constant, L_y is the side length of the system in the y direction, and ω is the frequency of the temporal oscillation of the shear flow.

In Fig. 4 we show the temporal evolution of the characteristic wave number $\langle k(t)\rangle$ for the same system as in Fig. 2(a), where an external shear flow with various frequencies is imposed. The parameters characterizing the shear flow are taken to be $\omega=$ 1.0, 0.5, 0.2, and 0.1 for Figs. 4(a), 4(b), 4(c), and 4(d), respectively, while $\dot{\gamma}_0=0.1$ is kept constant. The oscillations of the curves are due to the external periodic shear (42). Comparing Fig. 4(a) with Fig. 2(a), one recognizes that the shear flow with a high frequency $\omega=1.0$ does not give appreciable effects on the phase-separation dynamics. In this case, as the frequency ω is so large that the effects of the stretching of the block copolymer chains are not accumulated enough to make the perturbation effects enhanced. On the other hand, when we use a shear flow with smaller frequency ω as shown in Figs. 4(b)–4(d), the effect of chain stretching becomes important. In Fig. 4(b) we recognize that the case with the perturbation terms (dashed curve) relaxes much faster than the case without the perturbation terms (solid curves). In Fig. 4(c) the systems show complicated behavior that results from the competition between the external shear deformation and the internal relaxation due to the segment diffusion. Finally, in the case with the smallest frequency [Fig. 4(d)], the system with the perturbation terms (dashed curve) relaxes to a final domain structure that is different from that of the system without the perturbation terms (solid curve). In this case, the final domain structure of the case with the perturbation terms (dashed curve) is an almost regular lamellar structure in which the lamellar layers are aligned in the direction parallel to the external shear flow. Thus the extra relaxation (perturbation terms) associated with the chain stretching enhances the relaxation of the defects in the lamellar domain structures. These results indicate that the effect of the changes in the chain conformation is enhanced by the external shear deformation and the defects in the domain structure relax much faster.

E. Intuitive explanation of the simulation results

The simulation results presented in the previous subsections show that the changes in the chain conformation give a

non-negligible contribution to the ordering dynamics that accelerates the growth of domains. This acceleration of the domain growth can be understood by considering the relationship between the chain conformation and the hopping range of the kinetic kernel Λ. When the phase separation proceeds from the initial uniform state, composition fluctuations with a characteristic length scale of ξ emerge. Such composition fluctuations are described by nonzero order parameter $X(\mathbf{r})$, where regions with $X>0$ and regions with $X<0$ correspond to the A domains and B domains, respectively. As the A subchain and the B subchain of the block copolymer are attracted by the A domain and the B domain, the block copolymer chain is stretched when there is a gradient of the order parameter $X(\mathbf{r})$. Equations (8)–(10) indicate that the characteristic hopping range of the kinetic kernel is given by the end-to-end distance of each subchain. Thus the hopping range of the kinetic kernel is enlarged when the block copolymer chain is stretched due to the local gradient of the order parameter. This enlargement of the hopping range is expressed by the last term on the right-hand side of Eq. (28). (The perturbation term with $\langle H_1^2\rangle_0$ in the first term is merely a normalization factor over the entire system and it does not have a local nature.) The enlargement of the hopping range makes the segments easier to diffuse, which accelerates the phase separation and accelerates the relaxation of the defects in the domain structures, the latter effect being important in the ordering dynamics under the shear deformation shown in Fig. 4.

IV. CONCLUSION

In this paper we investigated the effects of the changes in the chain conformation that are introduced into the time-dependent Ginzburg-Landau-type equation of motion through a perturbation expansion of the nonlocal kinetic coefficient around the Gaussian conformation. By computer simulations, we found non-negligible effects of the change in the chain conformation on the relaxation dynamics of the microphase-separated domain structures. This result shows the importance of including the microscopic information, such as the chain conformation, into the macroscopic model based on the continuum density variables.

An experimental check of the results presented in this work is rather difficult because the experimental data always contain the correction effects from the deformation of the polymer chains that are discussed in Sec. III. One possible way to check the deformation effect is a precise quantitative comparison between the experimental data and the results of numerical simulations where the chain deformation effects are taken into account. In order to construct a model that can be used for this purpose, one should rely on a direct and rigorous numerical calculation of the path integral that is coupled with the time-dependent Ginzburg-Landau-type model. Such a trial is now under way [22].

ACKNOWLEDGMENTS

The author would like to thank D. Andelman, K. Binder, H. Brand, M. Doi, R. Hasegawa, K. Kawasaki, T. Koga, K. Kremer, H. Kuni, T. Ohta, Y. Okabe, A. Onuki, H. Otsuka, H. Pleiner, F. Tanaka, H. Tanaka, X.-F. Yuan, and W. Zimmermann for many useful comments and discussions. Computations were done using the FUJITSU VPP Computer at the Institute of Solid State Physics, Tokyo University, Japan. The work was partially supported by the Scientific Research Fund of the Ministry of Education, Science, Sports and Culture of Japan and by Japan-Germany Research Project sponsored by JSPS.

APPENDIX: CALCULATION OF THE PERTURBATION EXPANSION

In this appendix, we present the details of the perturbation expansion in deriving Eq. (28). We expand Eq. (27) in a power series in H_1 and retain terms up to second order. Then we obtain

$$\begin{aligned} P_{\tau\tau'}(\mathbf{r},\mathbf{r}') = n_0[&\langle \delta(\mathbf{r}(\tau)-\mathbf{r})\delta(\mathbf{r}(\tau')-\mathbf{r}')\rangle_0 \\ &-\beta\langle \delta(\mathbf{r}(\tau)-\mathbf{r})\delta(\mathbf{r}(\tau')-\mathbf{r}')H_1\rangle_0 \\ &+\tfrac{1}{2}\beta^2\langle \delta(\mathbf{r}(\tau)-\mathbf{r})\delta(\mathbf{r}(\tau')-\mathbf{r}')H_1^2\rangle_0 \\ &+o(H_1^3)]/[1-\beta\langle H_1\rangle_0 \\ &+\tfrac{1}{2}\beta^2\langle H_1^2\rangle_0+o(H_1^3)], \end{aligned} \tag{A1}$$

where $\langle\ \rangle_0$ is the average over the Gaussian chain whose Hamiltonian is given by H_0.

It is easy to show that

$$\langle H_1\rangle_0 = 0, \tag{A2}$$

which originates from the symmetric composition of the block copolymer under consideration. Using this result, Eq. (A1) can be rewritten as

$$\begin{aligned} P_{\tau\tau'}(\mathbf{r},\mathbf{r}') = n_0&\langle \delta(\mathbf{r}(\tau)-\mathbf{r})\delta(\mathbf{r}(\tau')-\mathbf{r}')\rangle_0 \\ &-n_0\beta\langle \delta(\mathbf{r}(\tau)-\mathbf{r})\delta(\mathbf{r}(\tau')-\mathbf{r}')H_1\rangle_0 \\ &+\tfrac{1}{2}n_0\beta^2[\langle \delta(\mathbf{r}(\tau)-\mathbf{r})\delta(\mathbf{r}(\tau')-\mathbf{r}')H_1^2\rangle_0 \\ &-\langle \delta(\mathbf{r}(\tau)-\mathbf{r})\delta(\mathbf{r}(\tau')-\mathbf{r}')\rangle_0\langle H_1^2\rangle_0] \\ &+o(H_1^3). \end{aligned} \tag{A3}$$

We introduce the Fourier transform of any functions of the form $R(\mathbf{r})$ and $P(\mathbf{r},\mathbf{r}')$ by

$$R(\mathbf{q}) = \mathcal{F}[R(\mathbf{r})](\mathbf{q}) = \int d\mathbf{r} R(\mathbf{r})\exp[i\mathbf{q}\cdot\mathbf{r}],$$

$$P(\mathbf{q},\mathbf{q}') = \mathcal{F}[P(\mathbf{r},\mathbf{r}')](\mathbf{q},\mathbf{q}') = \int d\mathbf{r}\int d\mathbf{r}' P(\mathbf{r},\mathbf{r}') \times\exp[i(\mathbf{q}\cdot\mathbf{r}+\mathbf{q}'\cdot\mathbf{r}')]. \tag{A4}$$

Then, we find

$$\langle H_1^2\rangle_0 = \frac{1}{(2\pi)^d V}\int d\mathbf{q}|\psi(\mathbf{q})|^2\left[\frac{12N}{b^2q^2}+2\left(\frac{6}{b^2q^2}\right)^2\right.$$

$$\times\{\eta_N(\mathbf{q})-4\eta_{N/2}(\mathbf{q})\}\Big], \tag{A5}$$

where d is the dimensionality of the system, V is the system volume, $q\equiv|\mathbf{q}|$, $\psi(\mathbf{q})$ is the Fourier transform of $\psi(\mathbf{r})$ defined in Eq. (24), and $\eta_\tau(\mathbf{q})$ is the Fourier transform of the density correlation function between two segments separated by τ on a Gaussian chain defined for $d=3$ by

$$\eta_\tau(\mathbf{q})=1-\exp(-\tfrac{1}{6}\tau b^2q^2). \tag{A6}$$

The other terms in Eq. (A3) are very complex. Using the definitions of the Fourier transform in Eq. (A4), we can rewrite Eq. (A3) as

$$\begin{aligned}P_{\tau\tau'}(\mathbf{q},\mathbf{q}')=&\frac{n_0(2\pi)^d}{V}\left(1-\frac{1}{2}\beta^2\langle H_1^2\rangle_0\right)\delta(\mathbf{q}+\mathbf{q}')h_{|\tau-\tau'|}(\mathbf{q})\\&-\frac{n_0\beta}{(2\pi)^d}\mathcal{I}_{\tau\tau'}(\mathbf{q},\mathbf{q}')+\frac{n_0\beta^2}{2(2\pi)^{2d}}\mathcal{J}_{\tau\tau'}(\mathbf{q},\mathbf{q}')\\&+o(H_1^3),\end{aligned} \tag{A7}$$

where h_τ, $\mathcal{I}_{\tau\tau'}(\mathbf{q},\mathbf{q}')$, and $\mathcal{J}_{\tau\tau'}(\mathbf{q},\mathbf{q}')$ are defined by

$$\begin{aligned}h_\tau(\mathbf{q})&=\exp[-\tfrac{1}{6}\tau b^2q^2],\\\mathcal{I}_{\tau\tau'}(\mathbf{q},\mathbf{q}')&=\mathcal{F}[\langle\delta(\mathbf{r}(\tau)-\mathbf{r})\delta(\mathbf{r}(\tau')-\mathbf{r}')H_1\rangle_0](\mathbf{q},\mathbf{q}'),\\\mathcal{J}_{\tau\tau'}(\mathbf{q},\mathbf{q}')&=\mathcal{F}[\langle\delta(\mathbf{r}(\tau)-\mathbf{r})\delta(\mathbf{r}(\tau')-\mathbf{r}')H_1^2\rangle_0](\mathbf{q},\mathbf{q}').\end{aligned} \tag{A8}$$

Substituting Eq. (A7) into Eqs. (14) and (15) and performing some straightforward algebra using the Gaussian statistics, we find that only the following quantities are contributing to $P_{\tau\tau'}(\mathbf{q},\mathbf{q}')$:

$$\begin{aligned}\mathcal{I}_{00}(\mathbf{q},\mathbf{q}')&=-\mathcal{I}_{NN}(\mathbf{q},\mathbf{q}')=-\frac{1}{V}\int d\mathbf{k}\psi(\mathbf{k})\delta(\mathbf{q}+\mathbf{q}'-\mathbf{k})\\&\quad\times I_2\left(\mathbf{0},-\mathbf{k};\frac{N}{2}\right),\end{aligned}$$

$$\begin{aligned}\mathcal{I}_{0N}(\mathbf{q},\mathbf{q}')&=-\mathcal{I}_{N0}(\mathbf{q},\mathbf{q}')=\frac{1}{V}\int d\mathbf{k}\psi(\mathbf{k})\delta(\mathbf{q}+\mathbf{q}'-\mathbf{k})\\&\quad\times I_2\left(-\mathbf{q},\mathbf{q}';\frac{N}{2}\right),\end{aligned}$$

$$\mathcal{I}_{(N/2)(N/2)}(\mathbf{q},\mathbf{q}')=0,$$

$$\begin{aligned}\mathcal{I}_{0(N/2)}(\mathbf{q},\mathbf{q}')&=-\mathcal{I}_{N(N/2)}(\mathbf{q},\mathbf{q}')\\&=-\frac{1}{V}\int d\mathbf{k}\psi(\mathbf{k})\delta(\mathbf{q}+\mathbf{q}'-\mathbf{k})\\&\quad\times\left[I_1\left(-\mathbf{q},\mathbf{q}';\frac{N}{2}\right)-h_{N/2}(\mathbf{q})I_1\left(\mathbf{0},\mathbf{k};\frac{N}{2}\right)\right],\end{aligned}$$

$$\begin{aligned}\mathcal{I}_{(N/2)0}(\mathbf{q},\mathbf{q}')&=-\mathcal{I}_{(N/2)N}(\mathbf{q},\mathbf{q}')\\&=-\frac{1}{V}\int d\mathbf{k}\psi(\mathbf{k})\delta(\mathbf{q}+\mathbf{q}'-\mathbf{k})\\&\quad\times\left[I_1\left(-\mathbf{q}',\mathbf{q};\frac{N}{2}\right)-h_{N/2}(\mathbf{q}')I_1\left(\mathbf{0},\mathbf{k};\frac{N}{2}\right)\right],\end{aligned} \tag{A9}$$

and

$$\begin{aligned}\mathcal{J}_{00}(\mathbf{q},\mathbf{q}')=\mathcal{J}_{NN}(\mathbf{q},\mathbf{q}')&=\frac{2}{(2\pi)^dV}\int d\mathbf{k}\int d\mathbf{k}'\psi(\mathbf{k})\psi(\mathbf{k}')\\&\quad\times\delta(\mathbf{q}+\mathbf{q}'-\mathbf{k}-\mathbf{k}')J(-\mathbf{k}-\mathbf{k}',-\mathbf{k},\mathbf{0};N),\end{aligned}$$

$$\begin{aligned}\mathcal{J}_{0N}(\mathbf{q},\mathbf{q}')=\mathcal{J}_{N0}(\mathbf{q},\mathbf{q}')&=\frac{2}{(2\pi)^dV}\int d\mathbf{k}\int d\mathbf{k}'\psi(\mathbf{k})\psi(\mathbf{k}')\\&\quad\times\delta(\mathbf{q}+\mathbf{q}'-\mathbf{k}-\mathbf{k}')J(\mathbf{q}'-\mathbf{k}-\mathbf{k}',\mathbf{q}'-\mathbf{k},\mathbf{q}';N),\end{aligned}$$

$$\begin{aligned}\mathcal{J}_{(N/2)(N/2)}(\mathbf{q},\mathbf{q}')&=\frac{2}{(2\pi)^dV}\int d\mathbf{k}\int d\mathbf{k}'\psi(\mathbf{k})\\&\quad\times\psi(\mathbf{k}')\delta(\mathbf{q}+\mathbf{q}'-\mathbf{k}-\mathbf{k}')\\&\quad\times\left[2J_1\left(\mathbf{0},\mathbf{k}',\mathbf{k}+\mathbf{k}';\frac{N}{2}\right)\right.\\&\quad\left.+\frac{1}{2}J_2\left(\mathbf{k},\mathbf{0},\mathbf{k}';\frac{N}{2}\right)\right],\end{aligned}$$

$$\begin{aligned}\mathcal{J}_{0(N/2)}(\mathbf{q},\mathbf{q}')=\mathcal{J}_{N(N/2)}(\mathbf{q},\mathbf{q}')&=\frac{2}{(2\pi)^dV}\int d\mathbf{k}\int d\mathbf{k}'\psi(\mathbf{k})\\&\quad\times\psi(\mathbf{k}')\delta(\mathbf{q}+\mathbf{q}'-\mathbf{k}-\mathbf{k}')\\&\quad\times\left[J_1\left(-\mathbf{q},\mathbf{k}'-\mathbf{q},\mathbf{q}';\frac{N}{2}\right)\right.\\&\quad+h_{N/2}(\mathbf{q})J_2\left(\mathbf{0},\mathbf{k}',\mathbf{k}+\mathbf{k}';\frac{N}{2}\right)\\&\quad\left.+\frac{1}{2}J_3\left(-\mathbf{q},\mathbf{k}-\mathbf{q},-\mathbf{k}';\frac{N}{2}\right)\right],\end{aligned}$$

$$\begin{aligned}\mathcal{J}_{(N/2)0}(\mathbf{q},\mathbf{q}')=\mathcal{J}_{(N/2)N}(\mathbf{q},\mathbf{q}')&=\frac{2}{(2\pi)^dV}\int d\mathbf{k}\int d\mathbf{k}'\psi(\mathbf{k})\\&\quad\times\psi(\mathbf{k}')\delta(\mathbf{q}+\mathbf{q}'-\mathbf{k}-\mathbf{k}')\\&\quad\times\left[J_1\left(-\mathbf{q}',\mathbf{k}'-\mathbf{q}',\mathbf{q};\frac{N}{2}\right)\right.\\&\quad+h_{N/2}(\mathbf{q}')J_2\left(\mathbf{0},\mathbf{k}',\mathbf{k}+\mathbf{k}';\frac{N}{2}\right)\\&\quad\left.+\frac{1}{2}J_3\left(-\mathbf{q}',\mathbf{k}-\mathbf{q}',-\mathbf{k}';\frac{N}{2}\right)\right],\end{aligned} \tag{A10}$$

where we defined the functions

$$I_1(\mathbf{q}_1,\mathbf{q}_2;N)=\frac{6}{b^2(q_1^2-q_2^2)}[h_N(\mathbf{q}_1)-h_N(\mathbf{q}_2)],$$

$$I_2(\mathbf{q}_1,\mathbf{q}_2;N)=\frac{6}{b^2(q_1^2-q_2^2)}[h_N(\mathbf{q}_1)-h_N(\mathbf{q}_2)]^2,$$

$$J_1(\mathbf{q}_1,\mathbf{q}_2,\mathbf{q}_3;N)=\frac{6}{b^2(q_1^2-q_2^2)}[I_1(\mathbf{q}_1,\mathbf{q}_3;N)-I_1(\mathbf{q}_2,\mathbf{q}_3;N)],$$

$$J_2(\mathbf{q}_1,\mathbf{q}_2,\mathbf{q}_3;N)=-2I_1(\mathbf{q}_1,\mathbf{q}_2;N)I_1(\mathbf{q}_2,\mathbf{q}_3;N),$$

$$J_3(\mathbf{q}_1,\mathbf{q}_2,\mathbf{q}_3;N)=-2I_1(\mathbf{q}_1,\mathbf{q}_2;N)I_1(\mathbf{0},\mathbf{q}_3;N),$$

$$J(\mathbf{q}_1,\mathbf{q}_2,\mathbf{q}_3;N)=J_1(\mathbf{q}_1,\mathbf{q}_2,\mathbf{q}_3;N)+J_2(\mathbf{q}_1,\mathbf{q}_2,\mathbf{q}_3;N). \tag{A11}$$

Then $\Lambda(\mathbf{q},\mathbf{q}')$ given in Eq. (14) is rewritten as

$$\Lambda(\mathbf{q},\mathbf{q}')=\frac{n_0(2\pi)^d}{2V}\left(1-\frac{1}{2}\beta^2\langle H_1^2\rangle_0\right)\{4\eta_{N/2}(\mathbf{q})-\eta_N(\mathbf{q})\}\times\delta(\mathbf{q}+\mathbf{q}')+\frac{n_0\beta^2}{4}[\mathcal{J}_{00}(\mathbf{q},\mathbf{q}')+2\times\mathcal{J}_{(N/2)(N/2)}(\mathbf{q},\mathbf{q}')+\mathcal{J}_{0N}(\mathbf{q},\mathbf{q}')-2\mathcal{J}_{0(N/2)}(\mathbf{q},\mathbf{q}')-2\mathcal{J}_{(N/2)0}(\mathbf{q},\mathbf{q}')]-\frac{n_0\beta^2V}{2(2\pi)^d}\int d\mathbf{k}\frac{1}{\eta_N(\mathbf{k})}[\mathcal{I}_{00}(\mathbf{q},\mathbf{k})-2\mathcal{I}_{(N/2)0}(\mathbf{q},\mathbf{k})-\mathcal{I}_{0N}(\mathbf{q},\mathbf{k})][\mathcal{I}_{00}(-\mathbf{k},\mathbf{q}')-2\mathcal{I}_{0(N/2)}(-\mathbf{k},\mathbf{q}')+\mathcal{I}_{0N}(-\mathbf{k},\mathbf{q}')]. \tag{A12}$$

This expression of Λ is not simple enough to be used for computer simulations. In order to simplify it, we adopt a long-wavelength approximation where only the leading terms in the expansion of the perturbation terms in power series in $\mathbf{q}$ and $\mathbf{q}'$ are retained. Then we obtain

$$\Lambda(\mathbf{q},\mathbf{q}')=\frac{n_0(2\pi)^d}{2V}\left(1-\frac{1}{2}\beta^2\langle H_1^2\rangle_0\right)\{4\eta_{N/2}(\mathbf{q})-\eta_N(\mathbf{q})\}\times\delta(\mathbf{q}+\mathbf{q}')+\frac{n_0\beta^2}{4(2\pi)^dV}\frac{b^4N^4}{216}\times\int d\mathbf{k}\psi(\mathbf{k})\psi(\mathbf{q}+\mathbf{q}'-\mathbf{k}')\times\{\mathbf{k}\cdot(-\mathbf{k}+\mathbf{q}+\mathbf{q}')\}(\mathbf{q}\cdot\mathbf{q}')+\cdots, \tag{A13}$$

where $\langle H_1^2\rangle_0$ is now expanded in wave number to give Eq. (31). Substituting this equation into Eq. (11), we finally obtain Eq. (28).

[1] *Physics of Complex and Supermolecular Fluids*, edited by S. A. Safran and N. A. Clark (Wiley, New York, 1987).
[2] *Micelles, Membranes, Microemulsions and Monolayers*, edited by W. M. Gelbart, A. Ben-Shaul, and D. Roux (Springer, Berlin, 1993).
[3] G. Gompper and M. Schick, in *Phase Transitions and Critical Phenomena*, edited by C. Domb and J. L. Lebowitz (Academic, London, 1994), Vol. 16.
[4] T. Kawakatsu, K. Kawasaki, M. Furusaka, H. Okabayashi, and T. Kanaya, J. Phys.: Condens. Matter **6**, 6385 (1994).
[5] K. Binder, J. Chem. Phys. **79**, 6387 (1983).
[6] K. Kawasaki and K. Sekimoto, Physica A **148**, 361 (1988).
[7] F. W. Wiegel, *Introduction to Path-Integral Methods in Physics and Polymer Science* (World Scientific, Singapore, 1986).
[8] G. J. Fleer, M. A. Cohen Stuart, J. M. H. M. Scheutjens, T. Cosgrove, and B. Vincent, *Polymers at Interfaces* (Chapman and Hall, London, 1993).
[9] E. Helfand and Z. R. Wasserman, Macromolecules **9**, 879 (1976).
[10] K. M. Hong and J. Noolandi, Macromolecules **14**, 727 (1981).
[11] M. Doi and S. F. Edwards, *The Theory of Polymer Dynamics* (Oxford Science, New York, 1986).
[12] M. W. Matsen and M. Schick, Phys. Rev. Lett. **72**, 2660 (1994).
[13] R. Israels, D. Jasnow, A. C. Balazs, L. Guo, G. Krausch, J. Sokolov, and M. Rafailovich, J. Chem. Phys. **102**, 8149 (1995).
[14] L. Leibler, Macromolecules **13**, 1602 (1980).
[15] T. Ohta and K. Kawasaki, Macromolecules **19**, 2621 (1986).
[16] G. H. Fredrickson and E. Helfand, J. Chem. Phys. **87**, 697 (1987).
[17] H. Fried and K. Binder, Europhys. Lett. **16**, 237 (1991).
[18] H. Fried and K. Binder, J. Chem. Phys. **94**, 8349 (1991).
[19] J. G. E. M. Fraaije, J. Chem. Phys. **99**, 9202 (1993).
[20] J. G. E. M. Fraaije, B. A. C. van Vlimmeren, N. M. Maurits, M. Postma, O. A. Evers, C. Hoffmann, P. Altevogt, and G. Goldbeck-Wood, J. Chem. Phys. **106**, 4260 (1997).
[21] R. Hasegawa and M. Doi, Macromolecules **30**, 3086 (1997).
[22] H. Kuni and T. Kawakatsu (unpublished).
[23] Y. Oono and S. Puri, Phys. Rev. A **38**, 434 (1988).
[24] M. Bahiana and Y. Oono, Phys. Rev. A **41**, 6763 (1990).
[25] T. Ohta, Y. Enomoto, J. L. Harden, and M. Doi, Macromolecules **26**, 4928 (1993); M. Doi, J. L. Harden, and T. Ohta, *ibid.* **26**, 4935 (1993).
[26] T. Koga and K. Kawasaki, Phys. Rev. A **44**, R817 (1991).
[27] A. Sariban and K. Binder, Macromolecules **24**, 578 (1991).
[28] K. Kremer (private communication).
[29] K. Kawasaki and T. Koga, Prog. Theor. Phys. Suppl. **99**, 339 (1989).
[30] R. Car and M. Parrinello, Phys. Rev. Lett. **55**, 2471 (1985).
[31] T. Taniguchi and A. Onuki, Phys. Rev. Lett. **77**, 4910 (1996).
[32] T. Kawakatsu, Phys. Rev. E **50**, 2856 (1994).
[33] Recently, a FFT method that is compatible with nonperiodic boundary conditions was presented by A. Onuki, J. Phys. Soc. Jpn. **66**, 1836 (1997).